Analysis of Effluent Gases during the CCVD Growth of Multi Wall Carbon Nanotubes from Acetylene

T. C. Schmitt[1*], A. S. Biris[2], D. W. Miller[1], A. R. Biris[3], D. Lupu[3],

S.Trigwell[4], Z. U. Rahman[5]

[1] National Center for Toxicological Research, Jefferson, Arkansas, 72079, U.S.A.

[2] University of Arkansas at Little Rock, Graduate Institute of Technology,

UALR Center of Nanotechnology, Little Rock, Arkansas, 72204, U.S.A.

[3] National Institute for Research and Development of Isotopic and Molecular Technologies,

P.O. Box 700, R-400293, Cluj-Napoca, Romania

[4] Electrostatics and Surface Physics Laboratory, Mail code: YA-C2-T,

Kennedy Space Center, NASA, FL 32899, U.S.A.

[5]Advanced Materials Processing and Analysis Center, University of Central Florida, 12443

Research Pkwy., Suite 304, Orlando, FL, 32826

* Corresponding author contact information

Email: tschmitt@nctr.fda.gov, Fax: 870-543-7980

Abstract

Catalytic chemical vapor deposition was used to grow multi-walled carbon nanotubes on a Fe:Co:$CaCO_3$ catalyst from acetylene. The influent and effluent gases were analyzed by gas chromatography and mass spectrometry at different time intervals during the nanotubes growth process in order to better understand and optimize the overall reaction. A large number of byproducts were identified and it was found that the number and the level for some of the carbon byproducts significantly increased over time. The $CaCO_3$ catalytic support thermally decomposed into CaO and CO_2 resulting in a mixture of two catalysts for growing the nanotubes, which were found to have outer diameters belonging to two main groups 8 to 35 nm and 40 to 60 nm, respectively.

Keywords: Catalytic Chemical Vapor Deposition, Carbon Nanotubes, Thermodynamic Analysis, Chromatography.

1.0 Introduction

Since their discovery by Iijima [1], the carbon nanotubes were intensively studied because of their very interesting electrical, mechanical, and optical properties. A large number of applications that involve carbon nanotubes (single walls or multi walls) were identified and developed over time but they all have a common need: nanotubes of high quality, high crystallization, and with little or no carbon byproducts such as amorphous carbon, graphite sheets, etc.

A number of methods have been used to grow carbon nanotubes including arc discharge [2], laser ablation methods [3, 4], and catalytic growth [5-8]. The most promising method however appears to be Catalytic Chemical Vapor Deposition (CCVD) because of the ability to more accurately control the reaction parameters [9-12]. By this process, a variety of liquid, solid, or gaseous carbon sources are introduced into the reaction zone over a catalyst at a controlled temperature [5-12]. A variety of catalyst systems can be employed, most of which involve transition metal particles (most often Fe, Co, Ni, etc) on oxidic supports, such as SiO_2, Al_2O_3, MgO, CaO, or zeolites [8,13-18]. Analysis of influent and effluent gases at various time points provides a way of monitoring the kinetics and phase of the reaction. In this paper, analysis of the effluent gas at several time intervals during the production of MWCNTs is described. Three different Gas Chromatographic Systems were employed in order to measure the utilization of acetylene feed gas and to identify other gases and volatile byproducts given off. These data were used to plot the kinetics of acetylene utilization and also to generate a schematic diagram of the reaction pathways of acetylene in correlation with the observed products.

2.0 Experimental

The nanotubes were grown from a Fe:Co:$CaCO_3$ catalyst, that was previously reported and developed and the reaction conditions were kept as previously described [9]. Approximately 100mg of catalyst was weighed and spread into a thin layer onto a graphite susceptor centered inside a quartz tube (27mm i.d. x 30mm o.d. x 980mm length) positioned horizontally inside of a resistive tube furnace. The quartz tube was purged with nitrogen at 200ml/min for 10 minutes to remove any traces of air before heat was applied. The furnace temperature was then set at the

2.1. Quantification of Acetylene by GC/FID

Acetylene levels were quantified using a Varian 3600 GC/FID equipped with a SPI temperature programmable injector. The GC column was a 50m x 0.53mm PLOT GS-Alumina (J&W Scientific/Agilent Technologies; Folsom, CA. U.S.A.). Helium at a flow rate of 6.5ml/min was used as carrier gas. The FID temperature was set at 200°C. A Precision Sampling Corp. 50µl series A-2 gas syringe from ChromTech was used to inject 10µl of sample gas into the instrument under the conditions described. The injector temperature began at 120°C and held for 0.10 minutes before increasing at a rate of 50°C/min. to a final temperature of 180°C where it was held for 0.50 minutes. At the time of injection, the column temperature was 100°C and held for 0.1 minutes before increasing at a rate of 5°C/min. to 150°C where it was held at this temperature for 1.9 minutes. The total run time was 12 minutes. Cryogenic cooling with CO_2 was used to bring the injector and column back to the original conditions quickly for the next sample injection. Under these conditions acetylene elutes at approximately 5 minutes and is the major peak observed in the chromatograms. Acetylene peak area was measured for each sample and the percentage relative to the control was calculated.

2.2. Light Hydrocarbons by GC/FID

The effluent hydrocarbon profiles were determined using the same Varian 3600 GC/FID system as described above. A Precision Sampling Corp. series A-2 gas syringe was used to inject 50 µl of sample gas. The injector temperature was initially 50°C and held for 0.10 minutes, then increased at a rate of 200°C/min. to 180°C and held for 4.25mins. At the time of

injection the column temperature was 45°C which was held for 3.0 minutes before increasing at 5°C/min. to 195°C and held at 195°C for 32mins. Total run time was 60 minutes per injection. Cryogenic cooling with CO_2 was used to bring the injector and column back to the original conditions for the next sample injection

2.3. GC/MS Analysis

Gas impurities and reaction by-products were identified using a Varian 3400 GC equipped with a SPI temperature programmable injector and Saturn GC/MS 2000 Ion Trap Detector. The column was a Varian Factor Four VF-5ms capillary (60m x 0.25 x 1μm). The carrier gas was helium at a head pressure of 20 psig. Ionization mode was 70eV electron impact. The mass range was scanned from m/z 38 to 155 at a rate of 0.25 seconds per scan from T_0 to 23 minutes. A Precision Sampling Corp. 50μl series A-2 gas syringe, pre-purged with helium, was used to inject either 10μl or 50μl of sample gas. The injection temperature was initially 50°C for 0.12 minutes, then increased at a rate of 200°C/min. to 200°C and held at that temperature for 1.0 minutes. The initial column temperature was 50°C and immediately increased at a rate of 5°C/minute to 70°C, then increased at 10°C/min. to 140°C, and then increased at 20°C/min. to 200°C, holding at 200°C for 1.0 minutes. Compound identification was made by comparison of peak spectra with the MS library and by direct examination. Standards containing acetone, benzene, and toluene vapor in helium were used to confirm the presents of these compound in the effluent gas by their retention time co-elution as well as by spectral matching.

2.4. GC/TCD Analysis

Samples were tested for the presence of free hydrogen using a packed column GC/TCD. The column was a 12' x 1/4" copper tube packed in-house with HayeSep A (100-120 mesh) GC column packing (Hayes Separations, Inc.). The column was prepared by cutting a 12 foot long section of ¼" copper tubing. The inside of the tubing was solvent cleaned with acetone and hexane and then, with argon flowing through the tube to prevent oxidation, heat cleaned using a propane torch. Once cooled, a silanized glass wool plug was placed in one end of the tube and HayesSep A was poured into the other end. A vibrating device and vacuum was used to settle the material in the tube. Once the tube was full to within about an inch of the top it was held in place using another silanized glass wool plug. The column was then coiled around a 4 in. diameter plexiglass tube and installed into the GC. The GC was a Varian 920 equipped with a Gow Mac thermal conductivity detector. The TCD filament current was set at 4 mA and powered by a Gow Mac Model 40-400 control unit. The output signal was monitored with a Shimadzu CR501 Chromatopac integrator. The injector, oven, and detector temperatures were held constant at 95°C, 40°C, and 100°C respectively. The carrier gas was nitrogen with a head pressure of 20 psig. Flow rates were 21.3ml/min and 2.85ml/min through the sample and reference filaments respectively. A reference standard of hydrogen was prepared by filling a 50ml septum capped syringe vial first with nitrogen to remove air and then with hydrogen to remove the nitrogen. Injections of as little as 5ul of reference hydrogen were detectable with the peak eluting in about 2.2 minutes.

2.5. Nanotubes Characterization

Characterization of the catalyst systems as well as of the resulting nanotubes were performed by a number of analytical means that include Transmission Electron Microscopy (HR TEM - FEI Tecnai F30 STEM), Scanning Electron Microscopy (SEM - JEOL 6400F SEM), Thermal Gravimetrical Analysis (Mettler Toledo TGA/SDTA 851°), Brunauer, Emmett, and Teller (BET) Surface Area Analysis by gas adsorption, and Raman Spectroscopy (Horiba Jobin Yvon LabRam) with 633 nm excitation.

3.0. Results and Discussions

Low and high resolution TEM images of the nanotubes as well as the corresponding 633 nm Raman spectra are shown in Figure 1 a, b, c. The low resolution TEM images were used to analyze the exterior diameter variation of the nanotubes, while the high resolution images were used to estimate the quality and the internal diameter of the nanotubes. It was observed that the carbon nanotubes exhibited outer diameters in two major ranges. Approximately 85% of the nanotubes had outer diameters between 8 to 35 nm while approximately 15% were in the range of 40 to 60 nm. Figure 2 is a histogram that shows the outer diameter distribution of the nanotubes. In general the tubes were well crystallized as shown by the HR TEM and Raman Spectroscopy. The Raman spectrum shows the D and G bands at 1329.2 and 1573.4 cm^{-1}, respectively. As shown before [19, 20], the D band is representative for the disordered carbon structures and defects, while the G band shows the graphitization and the crystalline properties of

Fig. 1.

Fig. 2.

The catalyst support ($CaCO_3$), was found to start decomposing thermally as the temperature reached 650°C into CaO and CO_2. Following the thermal decomposition process, the catalyst, Fe:Co:$CaCO_3$ = 2.5:2.5:95 wt % changed its composition to Fe:Co:CaO = 4.3:4.3:91.4 wt.%. The BET surface areas, measured by krypton adsorption, for the two catalysts are 6.2 m^2/g for the Fe:Co:$CaCO_3$ catalyst and 6.3 m^2/g for the Fe:Co:CaO catalyst, respectively and these results show that the two catalysts have basically the same surface areas. Figure 3 shows the isothermal mass decomposition of the Fe:Co:$CaCO_3$ catalyst at both 680°C and 800°C. At 700°C the $CaCO_3$ would be expected to decompose by 20 minutes, however under the experimental conditions it is possible that the decomposition was not complete. This would result in the co-existence of two catalyst systems for growing nanotubes and might explain the two main domains for the outer diameter of the carbon nanotubes as seen in Figure 2.

Fig. 3.

The effluent concentration of acetylene relative to the control as a function of reaction time was plotted and the results are illustrated in Figure 4. These measurements provide a means of determining the rate of utilization of acetylene and the efficiency of the reaction.

Fig. 4.

As the graph indicates, the effluent concentration of acetylene was very low between t_0 and 5 minutes followed by a slight increase at 8 minutes. This was expected in part due to the dead volume (~560ml) of the reaction chamber, the delay of acetylene getting to the collection tube and the strong catalytic process that takes place at the surface of the catalysts. The slope of the curve is almost flat between 8 and 14 minutes at which time the catalyst appears to be most efficient at utilizing acetylene. At 14 minutes, the residual acetylene concentration was about 15% that of the feed gas, by 20 minutes the level increased to nearly 40%, and by 26 minutes had climbed to roughly 80% that of the feed gas. The effluent acetylene levels at 32 and 38 minutes also had concentrations approximately 80% that of the feed gas. These results indicate that the reaction under these conditions is essentially complete after 20 to 25 minutes, after which time most of the acetylene is unused. A possible explanation for the very low rate of utilization after 26 minutes may be due to the build up of graphitic sheets and/or amorphous carbon around the catalyst particles which may prevent acetylene from reaching the catalyst or by poisoning the active catalytic sites.

The purity of affluent acetylene used throughout these experiments was analyzed and used as standard. The only one impurity found was small traces of acetone, which is normally used as a stabilizer. Analysis of the GC/MS chromatograms and spectral data revealed 8 hydrocarbon by-products attributable to the effluent gas. The majority of by-products identified were dimers, trimers, and tetramers of acetylene including such compounds as but-1-en-3-yne, benzene, and cycloocta-1,3,5,7-tetraene. Small amounts of additional compounds were also identified and include pent-3-en-1-yne, hexa-1,3-dien-5-yne, hexa-1,5-dien-3-yne, and toluene.

Injections of authentic standards of benzene, toluene, and acetone vapor in helium confirmed the presents of these compounds by the combined matching of peak retention times and fragmentation patterns. Also analysis of effluent gas samples collected at different stages of the reaction indicated that higher levels of byproducts were generated later in the reaction. Figure 5 shows a GC/MS total ion chromatogram of effluent gas collected from 17 to 20 minutes during the growth of MWCNTs.

Fig. 5.

A GC/FID chromatogram showing the hydrocarbon profile of an effluent gas sample collected from 35 to 38 minutes is shown in Figure 6. Other than acetylene, which eluted at 13.5 minutes, 12 additional peaks were observed in the reaction effluent that were not present in the control feed gas. Four peaks preceded acetylene, the first two of which appear to be methane and ethylene, respectively. The other two peaks which precede acetylene are relatively small and have not been identified. Eight additional peaks eluted after acetylene of which two, benzene and toluene, were positively identified by matching there peak retention times with the vapor of authentic standards. The other peaks are assumed to be the same as those observed by GC/MS. It was also observed by GC/FID that effluent gas samples collected at later stages of the reaction had higher levels of byproducts, particularly benzene, than those collected early in the reaction. Figure 7 shows the variation in benzene concentration as a function of time.

Fig. 6.

Fig. 7.

Injections of up to 2ml of effluent gas samples into the GC/TCD produced no detectable peak for hydrogen. This indicates that the molecular hydrogen (H_2) level, if any was present, was less than 0.25 percent by volume considering that a detectable peak could be seen from 5 µl injections of essentially pure hydrogen. Although our detection limit was so high, this does not necessarily prove that molecular hydrogen was not released but it does indicate that hydrogen is either not a major byproduct, enters in the formation of other types of hydrocarbon byproducts, or is used to reduce the catalysts surface.

Figure 8 shows a reaction scheme that helps clarify how the acetylene products might be produced. In addition to reacting with itself, it appears that acetylene is capable of reacting with low levels of acetone possibly through an enol form, or some other high temperature catalytic mechanism, which may explain the formation of the odd numbered 5 and 7 carbon compounds such as pent-3-en-1-yne and toluene. The small variations in the level of acetone in the effluent gas compared with the level contained in the affluent acetylene would support such a result, but in general the acetone is not believed to participate in the nanotubes growth process. The energy for the acetylene oligomerization and its decomposition into benzene was previously calculated as being -127.9 kcal/mol [21], and therefore the use of acetylene for growing carbon nanotubes will result in generation of various amounts of benzene. Figures 4 and 7, establish a direct correlation between the amount of unreacted acetylene that is collected in the effluent gases and the amount of benzene that is formed in the thermal decomposition of acetylene.

Fig. 8.

4.0. Conclusions

A study of the effluent gases from a CCVD process to grow multi wall carbon nanotubes was performed by using a number of gas chromatography techniques. It was found that the level of acetylene that is used during the nanotubes growth process decreases as the reaction advances. Developing methods to analyze, in real time, the effluent gases generated during such a reaction, could prove useful not just in monitoring the stage of the reaction, but also in controlling and adjusting its efficiency. Studying the amounts and types of gases produced provides clues to the overall reaction mechanisms. This will help lead to development of improved catalysts and reaction conditions for greater efficiency and utilization of carbon sources. It is apparent from both the GC/FID and GC/MS chromatograms that samples collected early in the reaction showed lower levels of some hydrocarbon by-products than those collected at later time points. Careful analysis of the effluent gasses provides the opportunity to examine the dynamics of nanotube growth and aid in minimizing the generation of undesired carbon byproducts. With the demand for nanotubes steadily increasing, both for research and for development of commercial applications, large scale reactions will require monitoring of effluent gases and byproducts from an economical as well as an environmental perspective. The development of in-line real time monitoring of influent and effluent gases will be crucial to providing more accurate information during production and scale up of the process for improved efficiency, methodology, and parametric control as well as helping to mitigate potential toxic effluents generated during large scale reactions. This along with better product characterization techniques that include

transmission electron microscopy (TEM), infrared and Raman spectroscopy, X-Ray Fluorescence (XRF), thermo-gravimetric analysis (TGA), differential scanning calorimetry (DSC), inductively couple plasma mass spectrometry ICP-MS, conductivity measurements and others will provide a means for standardization and quality control.

Acknowledgements

We would like to thank L.A.Groves for her assistance during collection of the reaction effluent samples and D.A. Buzatu , J.G. Wilkes, P. Marginean, and Z. Moldovan for useful discussions in preparing this manuscript.

References

[1]. Iijima S. Helical microtubules of graphitic carbon. Nature 1991; 353:56-58.

[2]. Journet C, Maser W K, Bernier P, Loiseau A, Lamy de la Chapelle M, Lefrant S, Deniard P, Lee R, Fisher JE. Large- scale production of single-walled carbon nanotubes by the electric arc technique. Nature 1997; 388:756–8.

[3]. Thess A, Lee R, Nikolaev P, Dai H, Petit P, Robert J, Xu C, Lee YH, Kim SG, Rinzler AG, Colbert DT, Scuseria GE, Tomanek D, Fischer J, Smalley RE. Crystalline ropes of metallic carbon nanotubes. Science 1996; 273:483–7.

[4]. Maser WK, Munoz E, Benito AM, Martinez M T, de la Fuente G F, Maniette Y, Anglaret E, Sauvajol J-L. Production of high density single-walled nanotube material by a simple laser-ablation method. Chem Phys Lett 1998; 292:587–93.

[5]. Dai H, Rinzler AG, Nikolaev P, Thess A, Colbert DT, Smalley RE. Single-wall nanotubes produced by metal-catalyzed disproportionation of carbon monoxide. Chem Phys Lett. 1996; 260:471–5.

[6]. Colomer JF, Bister G, Willems I, Konya Z, Fonseca A, Van Tendeloo G, Nagy JB. Synthesis of single-walled carbon nanotubes by catalytic decomposition of hydrocarbons. Chem Commun 1999; 14:1343–4.

[7]. Ando Y, Zhao X, Sugai T, Kumar M. Growing carbon nanotubes. Materials Today 2004, October:22-29.

[8]. Soneda Y, Duclaux L, Béquin F. Synthesis of high quality multi-walled carbon nanotubes from the decomposition of acetylene on iron-group metal catalysts supported on MgO. Carbon 2002; 40:965-969.

[9]. Couteau E, Hernardi K, Seo JW, Thiên-Nga L, Mikó Cs, Gaál R, Forró. CVD synthesis of high-purity multiwalled carbon nanotubes using $CaCO_3$ catalyst support for large-scale production. Chem. Phys. Lett. 2003; 378:9-17.

[10]. Lupu DM, Biris AR, Misan I, Lupsa N, Biris AS, Buzatu DA, Kleeve M. Growth of nanoscale carbon structures and their corresponding hydrogen uptake properties. Particulate Science and Technology: An International Journal 2002; 20:225-234.

[11]. Lupu D, Biriş AR, Jianu A, Bunescu C, Burkel E, Indrea E, Mihăilescu G, Pruneanu S, Olenic L, Mişan I. Carbon nanostructures produced by CCVD with induction heating. Carbon 2004; 42:503-507.

[12]. Okamoto A, Shinohara H. Control of diameter distribution of single-walled carbon nanotubes using the zeolite-CCVD method at atmospheric pressure. Carbon 2005; 43:431-436.

[13]. Piao L, Li Y, Chen J, Chang L, Lin JYS. Methane decomposition to carbon nanotubes and hydrogen on alumina supported nickel aerogel catalyst. Catalysis Today 2002; 74:145-155.

[14]. Kitiama B, Alvarez WE, Harwell JH, Resasco DE. Controlled production of single-wall carbon nanotubes by catalytic decomposition of CO on bimetallic Co-Mo catalysts. Chem Phys Lett 2000;317;497-503.

[15]. Zaikovskii VI, Chesnokov VV, Buyanov RA. The relationship between the state of active species in a Ni/Al_2O_3 catalyst and the mechanism of growth of filamentous carbon. Kinetics Catal. 2001; 42(6):813-820.

[16]. Liang Q, Gao LZ, Li Q, Tang SH, Liu BC, Yu ZL. Carbon nanotube growth on Ni-particles prepared in situ by reduction of La_2NiO_4. Carbon 2001; 39:897-903.

[17]. Sato S, Kawabata A, Nihei M, Awano Y. Growth of diameter-controlled carbon nanotubes using monodisperse nickel nanoparticles obtained with a differential mobility analyzer. Chem. Phys. Lett. 2003; 382:361-366.

[18]. Hernadi K, Kónya Z, Siska A, Kiss J, Oszkó A, Nagy JB. On the role of catalyst, catalyst support and their interaction in synthesis of carbon nanotubes by CCVD. Mater Chem Phys. 2002;77:536-41.

[19]. Dresselhaus MS, Dresselhaus G, Saito R, Jorio A. Raman spectroscopy of carbon nanotubes. Physics Reports.2005;409:47-99.

[20]. Lee CJ, Park J, Huh Y, Lee JY. Temperature effect on the growth of carbon nanotubes using thermal chemical vapor deposition. Chemical Physics Letters. 2001;343:33-38.

[21]. Bach RD, Wolber GJ, Schlegel HB. The Origin of the Barriers to Thermally Allowed, Six-Electron, Pericyclic Reactions: The Effect of HOMO-HOMO Interactions on the Trimerization of Acetylene. J. Am. Chem. Soc. 1985; 107, 2837-2841.

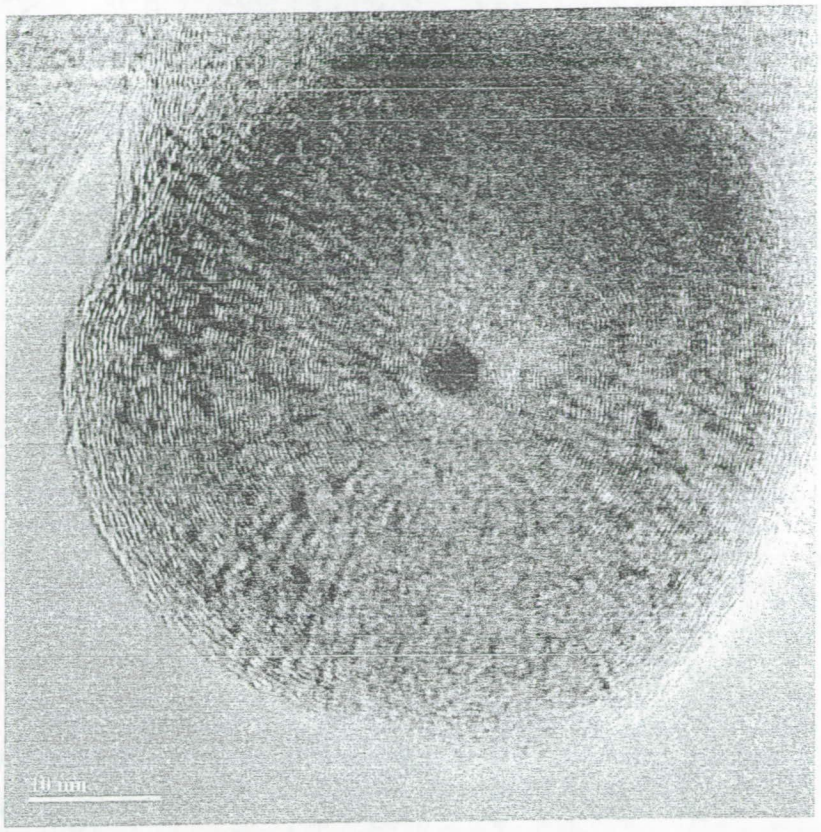

(d)

Fig. 1. Low (a), High (b) Resolution TEM pictures of the carbon nanotubes grown by CCVD on a Fe:Co:$CaCO_3$ catalyst as well as the corresponding 633 nm Raman Spectra showing the D and G bands (c). Figure 1 (d) is a HR TEM picture of an open end nanotube that shows its lumen. It can be observed the well crystallized concentrical walls around the nanotube lumen.

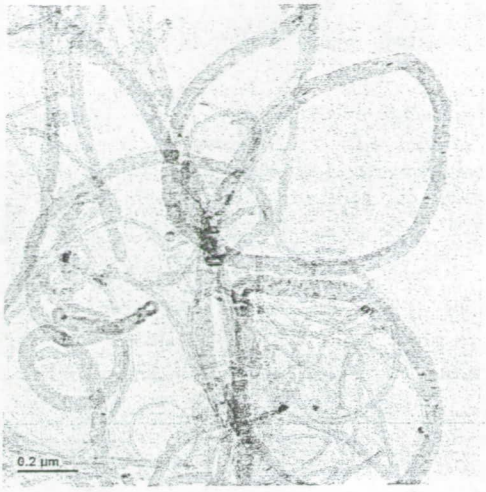
0.2 µm

(a)

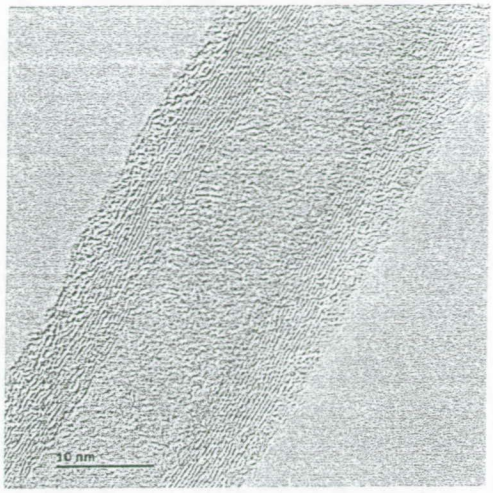
10 nm

(b)

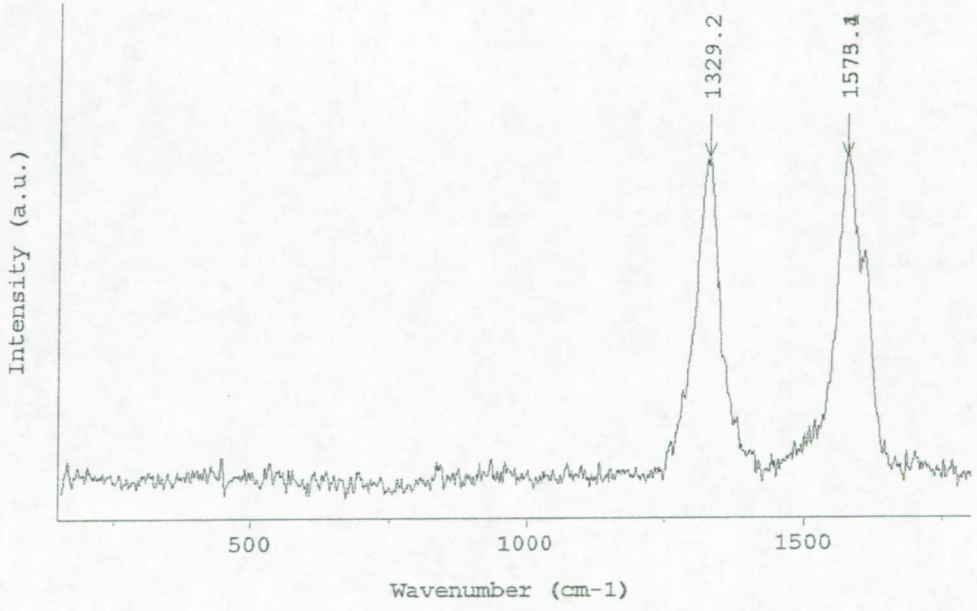
1329.2
1573.4
Intensity (a.u.)
500
1000
1500
Wavenumber (cm-1)

(c)

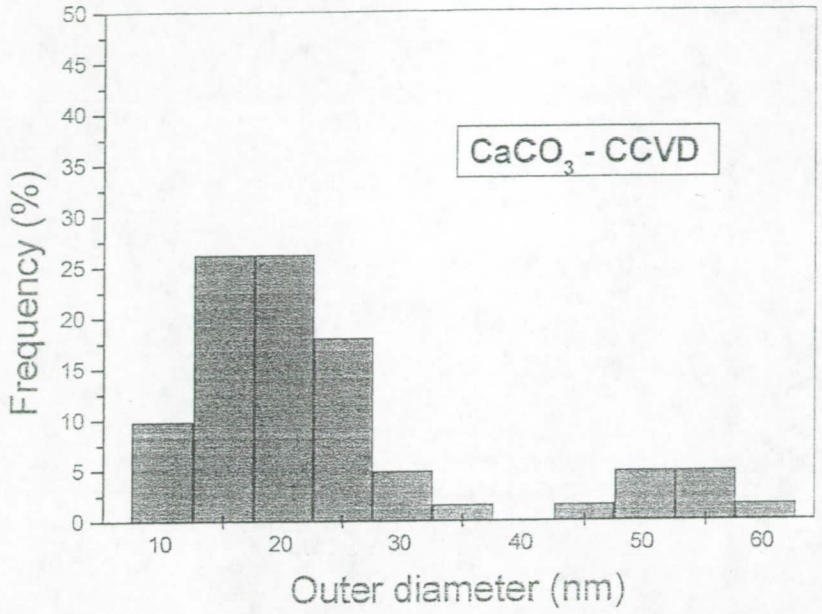

Fig. 2. Diameter distribution histogram for multi wall carbon nanotubes grown on the Fe:Co:$CaCO_3$ and Fe:Co:CaO catalysts.

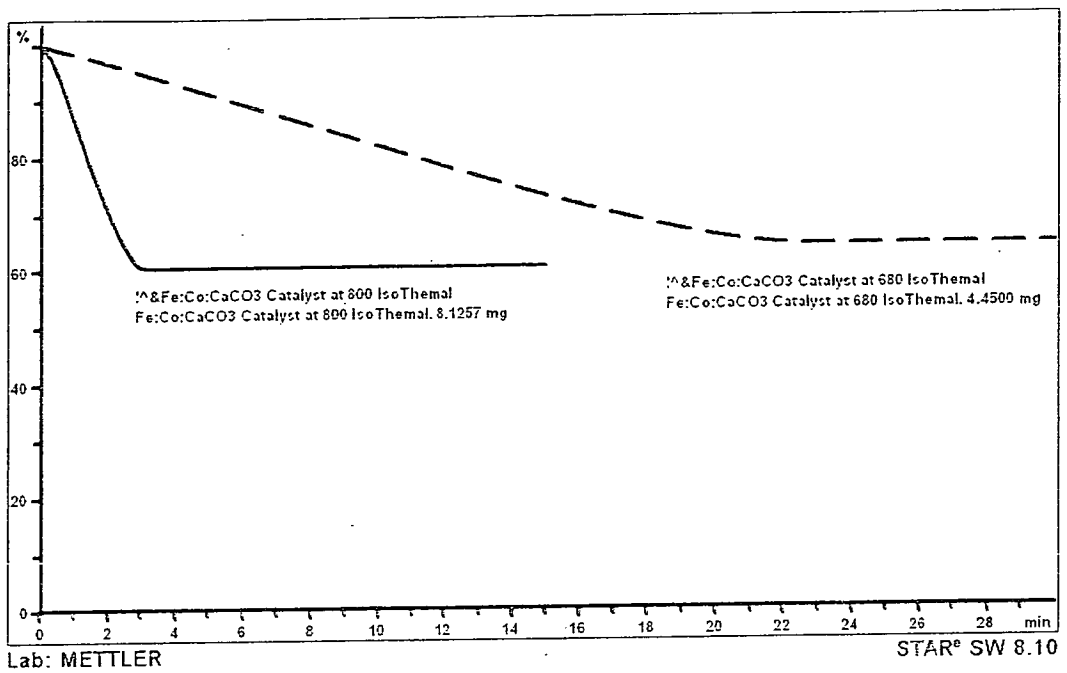

Fig. 3. The normalized isothermal mass decomposition of the Fe:Co:$CaCO_3$ catalyst at 680 and 800 °C

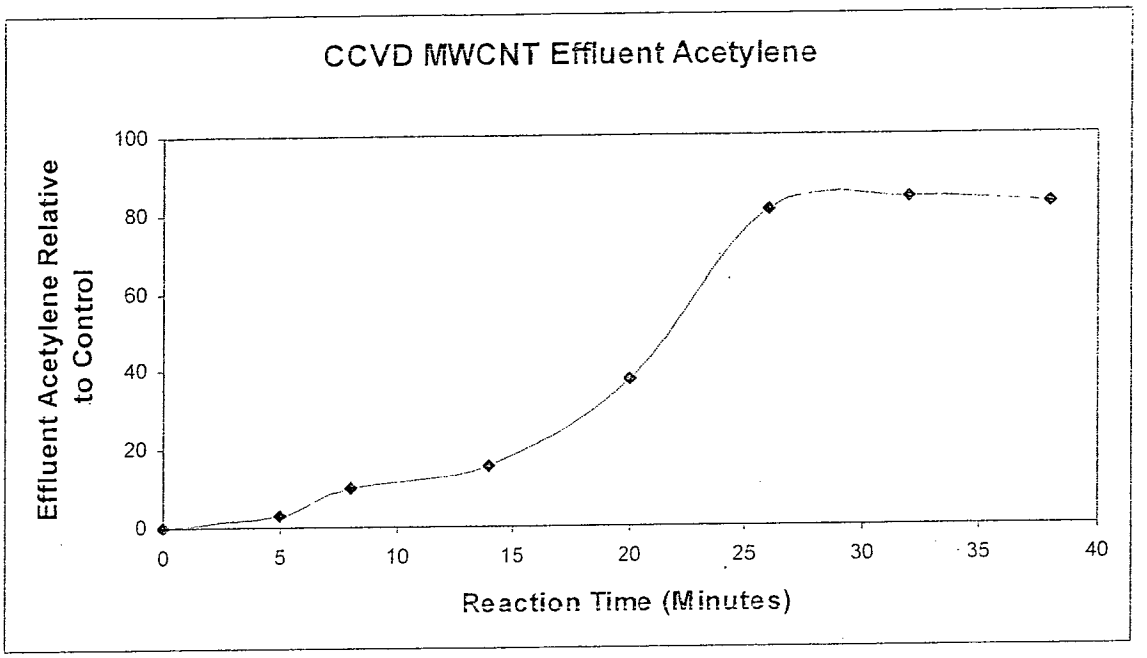

Fig. 4. Time variation of the effluent concentration of acetylene relative to the control. (Time points indicated represent the end of the 3 minute sampling time interval relative to t_0)

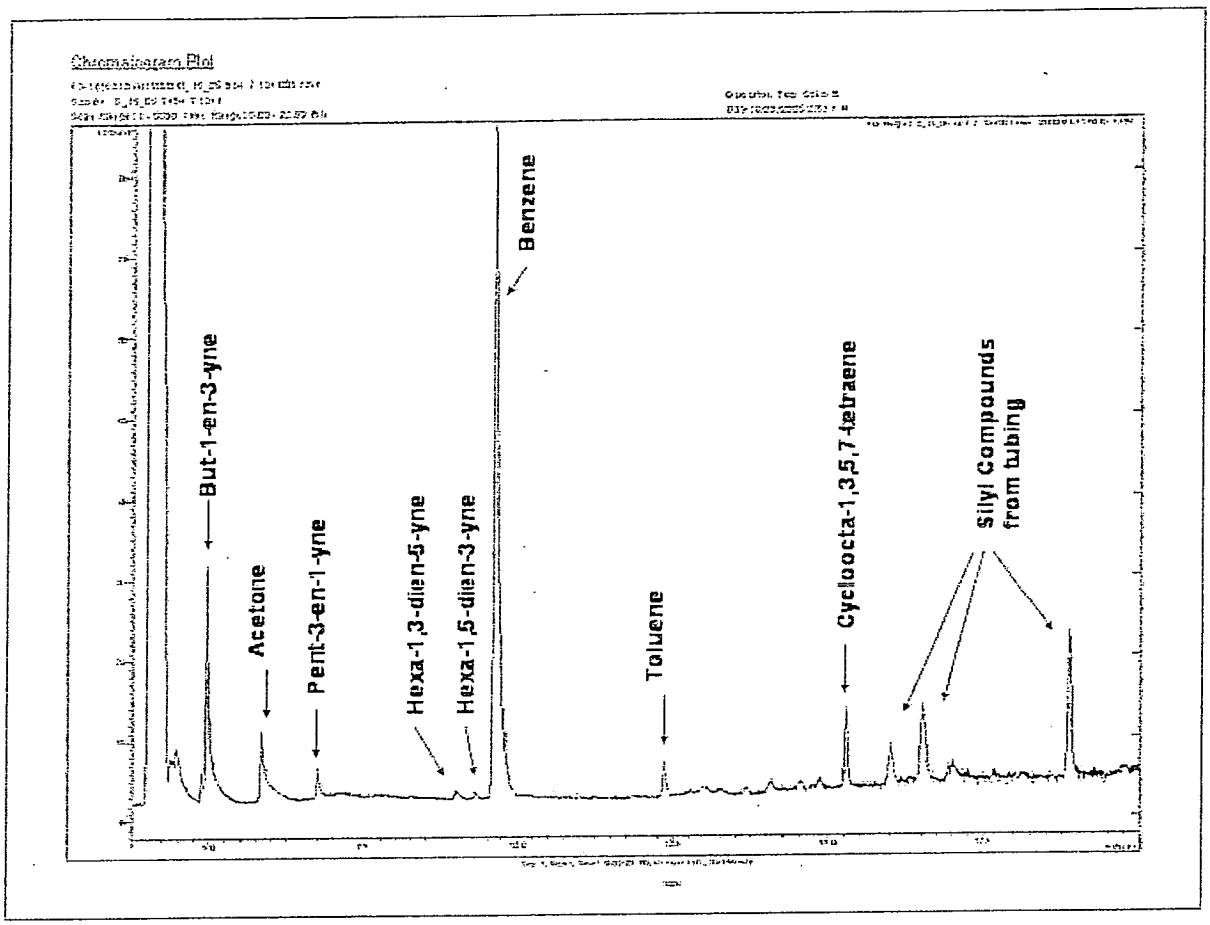

Fig. 5. GC/MS total ion chromatogram of effluent gas collected during production of MWCNTs. Acetone, benzene, and toluene were confirmed by standards. The other compounds were assigned names based on spectral library matching and their likelihood of formation.

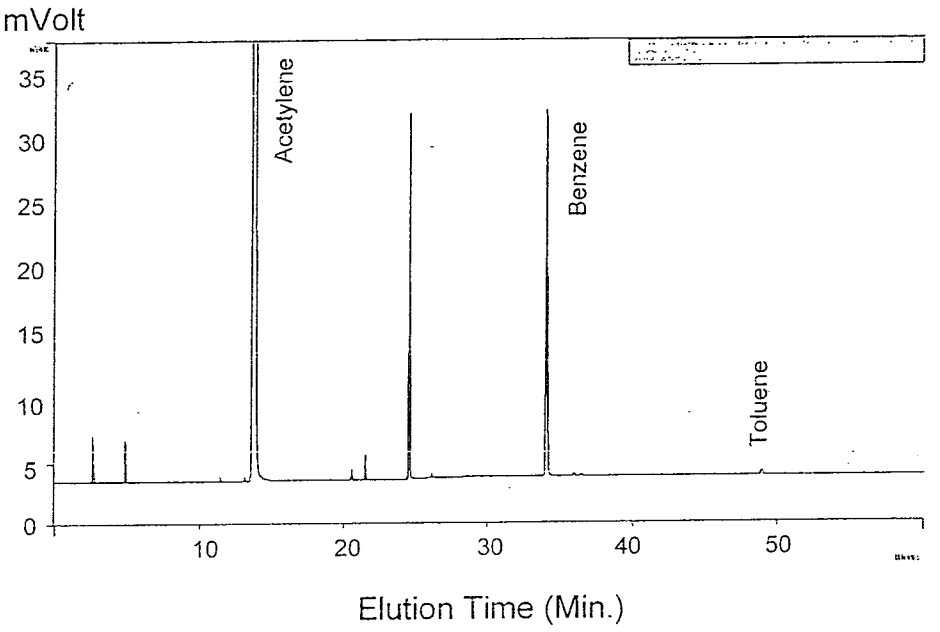

Fig. 6. GC/FID chromatogram of a gas sample collected from 35-38 minutes into the reaction.

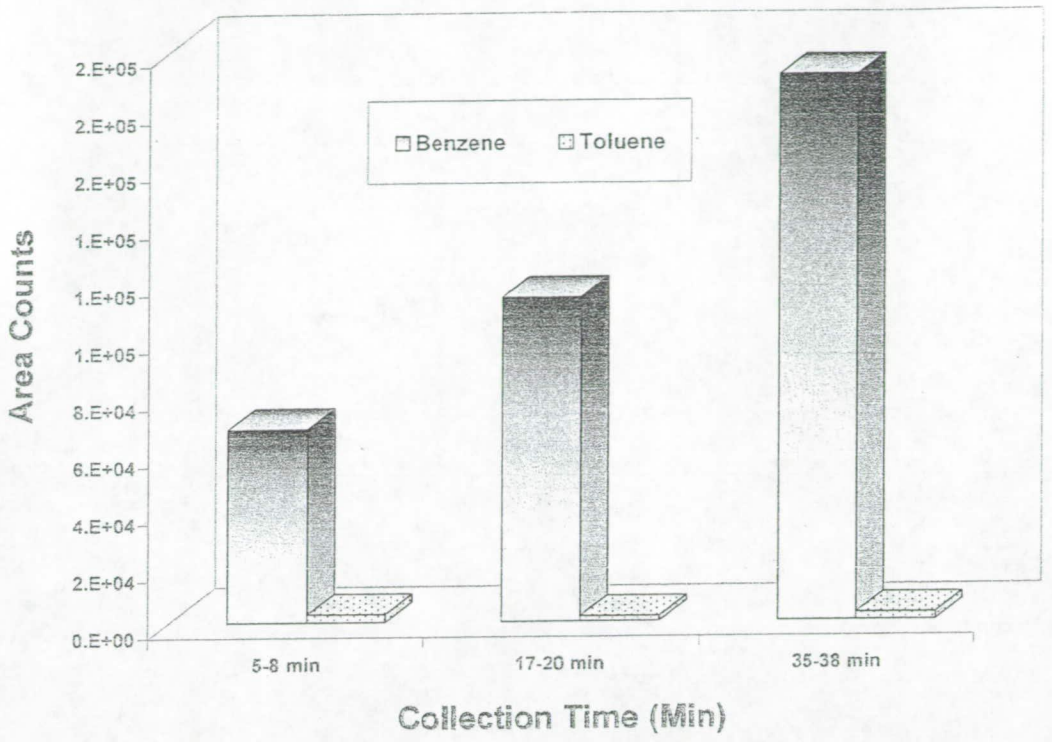

Fig. 7. Variation of benzene concentration in the effluent as a function of time as analyzed by GC/FID.

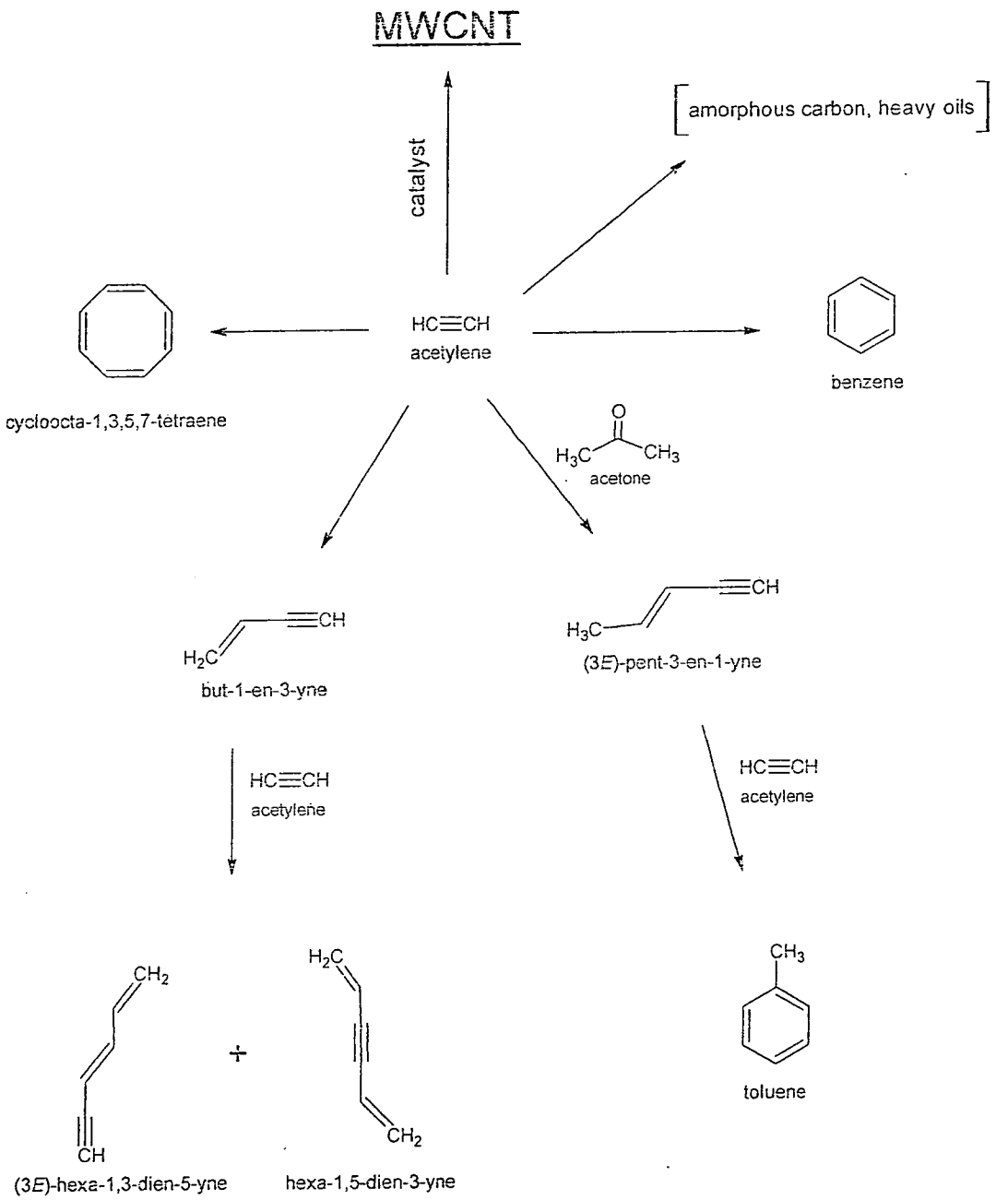

Fig. 8. Proposed reaction scheme for MWCNTs production that explains the formation of the observed by-products.